

Melting of Metastable Crystallites in Charge-Stabilized Colloidal Suspensions

Amy E. Larsen and David G. Grier

*The James Franck Institute and Department of Physics, The University of Chicago, 5640 South Ellis Avenue,
Chicago, Illinois 60637*

(Received 14 December 1995)

We use low-frequency electrophoresis to crystallize monodisperse charge-stabilized colloidal suspensions. Rather than reverting directly to their equilibrium fluid state when the field is removed, some suspensions retain long-lived metastable crystallites whose evolution we track using high-resolution digital video microscopy. To quantify the decay of order in this system we introduce an empirical criterion for distinguishing spheres in the crystal from those in the fluid. [S0031-9007(96)00209-8]

PACS numbers: 82.70.Dd, 64.60.My

Monodisperse charge-stabilized colloidal suspensions provide convenient model systems for studying the microscopic mechanisms of structural phase transitions such as freezing and melting. Depending on a suspension's volume fraction and counterion concentration, its ensemble of colloidal microspheres can undergo disorder-order transitions from fluid states to highly organized crystals of either face-centered cubic (fcc) or body-centered cubic (bcc) symmetry. These phase transitions are analogous to those induced in simple metals and noble gases by variations in pressure and temperature. Unlike the atoms in conventional materials, however, individual colloidal spheres are large enough to image directly with a conventional light microscope and move slowly enough to track with standard video equipment.

Direct imaging and light scattering studies have addressed metastability in the freezing of supercooled colloidal fluids [1] and equilibrium crystal-fluid coexistence [2]. The melting of colloidal crystals has received far less attention because of the comparative difficulty of creating a superheated crystalline state. In this Letter we describe a technique for creating superheated colloidal crystallites in contact with their fluid. To quantify the evolution of order during melting we introduce an empirical criterion which allows us to distinguish crystal from fluid with single-particle resolution. Under a range of experimental conditions, the measured ordering dynamics provide evidence for metastability in a strongly first-order melting transition. This behavior is surprising in a system whose pair-wise interactions are generally taken to be purely repulsive [3].

The colloidal suspension in this study consists of polystyrene sulphate spheres of radius $\sigma = 325 \pm 3$ nm suspended in water at volume fraction $\phi = 0.02$. These spheres have titratable surface charge densities of 1 electron equivalent per 10 nm^2 surface area. The mutual repulsion engendered by these surface charges stabilizes the suspension against flocculating under the influence of van der Waals attractions [3]. Dialysis against deionized water followed by tumbling with ion exchange resin reduces concentrations of dissolved polymer and stray ions

which might modify the charge-mediated interaction. The colloid is contained in a sample volume of dimensions $10 \times 20 \times 0.02 \text{ mm}^3$ created by sealing the edges of a cover slip to a microscope slide. Glass reservoir tubes extending from holes drilled through the slide provide access to the sample volume. Mixed bed ion exchange resin added to the tubes further reduces the concentration of stray ions leached from the glass surfaces. The open ends of the reservoir tubes are continuously flushed with humidified Ar to prevent contamination by airborne CO_2 . Changing the Ar pressure allows us to drive the suspension back and forth between the reservoirs to bring the system rapidly into chemical equilibrium at very low ionic strength.

The sealed cell is mounted on the stage of an Olympus IMT-2 inverted optical microscope. The microscope's $100\times$ N.A. 1.4 oil immersion objective provides a field of view of $54 \times 40 \mu\text{m}^2$ with a depth of focus of $\pm 0.200 \mu\text{m}$ which is comparable to a sphere diameter. The addition of a $5\times$ video eyepiece provides a magnification of 85 nm/pixel on the attached charge coupled device video camera. An individual sphere subtends an area of 20 pixels in this system and roughly 500 spheres are in focus in a given video frame. The colloidal spheres' motions are recorded on video tape at standard $1/30 \text{ s}$ intervals before being digitized and analyzed.

Creating superheated crystal requires introducing ordered regions into an equilibrium colloidal fluid. Such nonequilibrium ordering has been achieved through shear-induced alignment [4] and by the application of optical gradient forces [5]. The experimental geometries in the former class of experiments do not lend themselves to high resolution imaging, while the latter approach is only amenable to single-layer systems.

The response of a charge-stabilized suspension to an electric field provides another means to create transient ordered states. Negatively charged microspheres flow against the field through electrophoresis, while positively charged counterions at the glass sample container's Helmholtz layers flow with the field through electroosmosis. The surrounding water is set in motion through

viscous coupling to the ionic hydration spheres. These contributions together with volume-preserving counterflows result in a roughly parabolic flow profile as indicated in Fig. 1. A sphere driven through a shear flow experiences a Magnus force with a component perpendicular to the driving direction [6]. Such hydrodynamic forces are responsible for the accumulation of particles near container walls in fluidized beds [7]. We use a slowly oscillating electric field to compress colloidal spheres against the smooth parallel glass walls of our sample cell. The resulting increase in sphere density can be great enough to produce several polycrystalline surface layers while leaving the central volume of the container void of spheres.

The electric field is applied between thin film parallel plate gold electrodes patterned onto the sample cell as shown in Fig. 1. The spheres' motion under a 10 V/mm peak-to-peak field is slow enough to maintain laminar flow in the sample volume. Driving at 60 Hz phase locks the spheres' motions to the video camera's images and allows continuous monitoring of the crystallization process. By detuning to 59 Hz we measure the spheres' response to be roughly 1 diameter peak to peak along the system's midplane.

The compression-driven freezing transition occurs at both upper and lower walls; the data we present were obtained near the more accessible lower wall. The resulting multilayer fcc crystal presents its high density (111) face to the smooth rigid glass so that a single layer appears as an array of equilateral triangles. When the field is removed, the polycrystal first expands and then melts, starting along the grain boundaries and continuing until

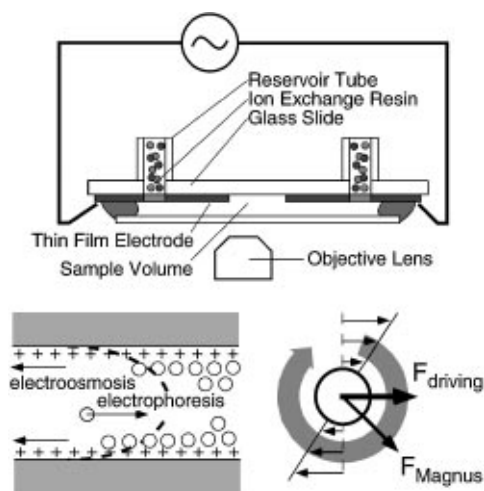


FIG. 1. (top) Schematic cross section of the colloid cell. The reservoir tubes are connected to the gas system which is not shown for clarity. (lower left) Cross-sectional view of electrostatic compression. The electric field produced by the thin film electrodes is directed from right to left in this drawing. (lower right) A colloidal sphere rotates in a shear flow. Rotational flow around the sphere engenders a Magnus force when the sphere is driven through the flow.

the entire suspension returns to the equilibrium fluid state. Less strongly interacting systems (those with counterion concentration on the order of $1 \mu M$ or greater) melt within seconds. More strongly interacting systems, however, can retain long-lived superheated crystallites such as the examples in Fig. 2 coexisting with the surrounding fluid for as long as an hour. Flowing less strongly interacting suspensions over ion exchange resin reduces the counterion concentration and reproducibly makes possible the creation of long-lived crystallites.

Metastable crystals drift freely across the glass surfaces, suggesting that inhomogeneities in the surfaces' properties are not responsible for their longevity. Direct sphere-wall interactions also are not likely to mediate metastable ordering as compression-crystallized monolayers are always unstable.

To quantify these observations, we introduce an empirical criterion for distinguishing crystalline sites from those in the fluid. We base this distinction on the six-fold bond-orientational order parameter originally introduced by Halperin and Nelson [8] in the context of

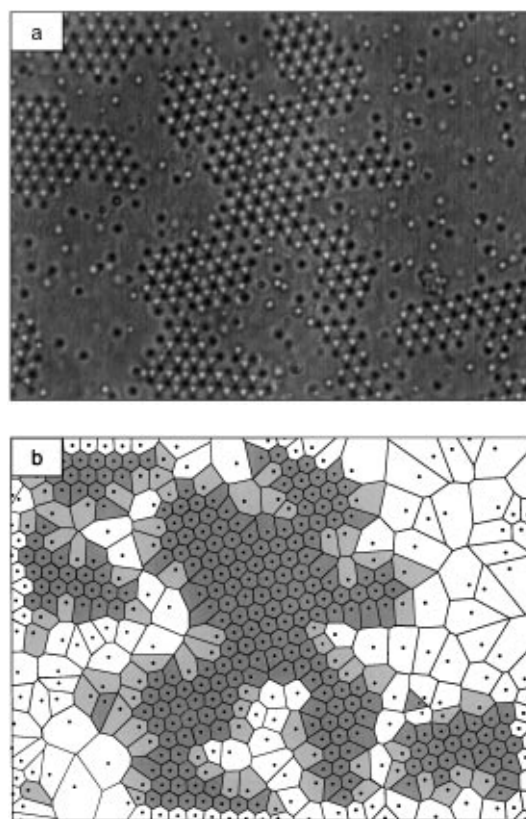


FIG. 2. (a) Metastable crystallites after melting for 15 min. Spheres' images change from bright to dark with increasing height above the focal plane. (b) Voronoi construction of the nearest neighborhoods for one layer of particles in (a). Each sphere location is indicated by a point. Crystalline neighborhoods are dark gray; surface sites are shaded light gray. Fluid regions and neighborhoods extending beyond the field of view are not shaded.

two-dimensional melting. For a site k whose nearest neighbors [9] labeled by j are arrayed at angles θ_{jk} from a reference direction, the sixfold bond-orientational order parameter is defined as

$$\psi_{6k} = \langle \exp(i6\theta_{kj}) \rangle_j, \quad (1)$$

where the angle brackets indicate an average over nearest neighbors. The magnitude $m_{6k} = |\psi_{6k}|$ achieves a maximum value of one for uniformly sixfold coordinated sites and is smaller for others. In practice, we find that m_6 does not provide sufficient information to distinguish unambiguously between crystals near melting and fluids near freezing. Additional insight into the degree of local orientational ordering is provided by the magnitude of the projection of ψ_{6k} onto the mean local orientation field

$$n_{6k} = |\psi_{6k}^* \langle \psi_{6j} \rangle_j|. \quad (2)$$

Measurements on suspensions in homogeneous fcc crystal and fluid phases such as those in Fig. 3 indicate that a site k can be classified as crystal if

$$m_{6k} + n_{6k} > 1. \quad (3)$$

We therefore use Eq. (3) as a practical criterion for distinguishing spheres in the ordered phase from those in or adjacent to the fluid. Because this criterion depends only on particles' instantaneous locations and not on their dynamics, it is useful for time-resolved studies of interfacial fluctuations. While Eq. (3) is specialized to the case of ordering in the (111) face of fcc crystals, other two- and three-dimensional generalizations are possible [10]. We avoid misidentifications due to measurement error in the particle locations by performing Monte Carlo refinements on the particle classifications using the calibrated 20 nm error in centroid location [11]. In addition to the core crystalline sites identified by Eq. (3), we label noncrystalline sites connected to the core by nearest-neighbor bonds [9] comparable in length to the crystal's lattice spacing as crystal surface sites. All other spheres are classed as belonging to the fluid. Typical classifications appear in Fig. 2(b).

The fraction of the field of view subtended by crystalline nearest neighborhoods provides a measure of the degree of in-plane crystalline ordering. Figure 4 shows the evolu-

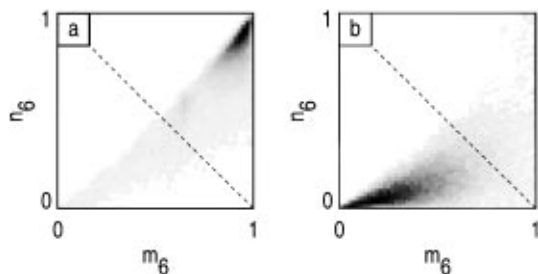


FIG. 3. Experimental probability distributions for the order parameters m_6 and n_6 in (a) polycrystalline and (b) fluid suspensions. The diagonal dashed lines indicate the empirical ordering criterion $m_6 + n_6 = 1$.

tion of the crystal fraction with time for two typical runs, one with rapid melting and another in which long-lived crystallites formed. In the former case the entire sample reverts to a fluid state in a matter of seconds. In the latter, the time scale for the phase transition extends to more than half an hour.

Although ionic strength affects the dynamics of the fluid state, this effect alone does not account for the observed dramatic difference in melting rates. We measure [11] the fluids' self-diffusion coefficients, D , by tracking mean square particle displacements, $\langle r^2 \rangle$, and fitting with the Einstein-Smoluchowsky equation, $\langle r^2 \rangle = 4Dt$. For the runs shown in Fig. 4, the precompression self-diffusion coefficients differ by no more than a factor of 2 ($D_{\text{fast}} = 0.24 \mu\text{m}^2/\text{s}$, $D_{\text{slow}} = 0.12 \mu\text{m}^2/\text{s}$) while their melting rates differ by 2 orders of magnitude. The time required for a sphere to diffuse the thickness of the sample volume provides a rough estimate of the diffusion-limited time to melting and is on the order of 10 s for either sample. This estimate agrees well with observed rates in rapidly melting samples. Furthermore, even the strongly interacting fluid is far from the equilibrium crystallization point as determined by the Löwen-Palberg-Simon (LPS) dynamical freezing criterion [12]. The LPS criterion states that a colloidal fluid will freeze when its self-diffusion coefficient falls below $D_c = 0.095D_0$, where $D_0 = 0.89kT/6\pi\eta\sigma = 0.63 \mu\text{m}^2/\text{s}$ is the wall-corrected [11] free-particle self-diffusion coefficient in water ($\eta = 1$ cP) at $T = 25^\circ\text{C}$. The more strongly interacting suspension is well above this threshold with $D_{\text{slow}} = 2D_c$.

The microstructure of the long-lived crystallites provides evidence that the ordered state is stabilized by a cohesive energy. While crystallites such as those in Fig. 2 are not compact, their well-defined facets bespeak a

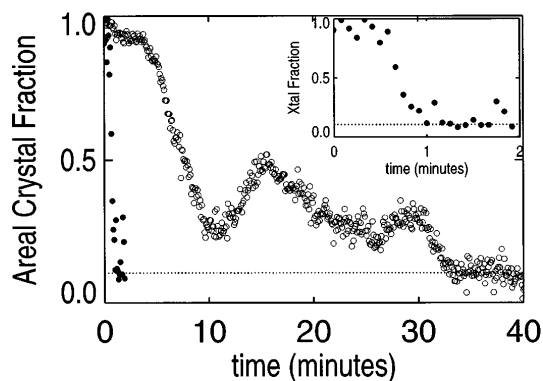


FIG. 4. Decay of crystalline ordering during melting. Filled circles correspond to the areal crystal fraction after electrophoretic compression in a suspension with moderately high ionic strength. Open circles show the equivalent result for a suspension of low ionic strength. The dashed line indicates the level of spontaneous order fluctuations in the equilibrium fluid. Fluctuations in the long-lived state reflect crystallites drifting through the field of view.

sizable surface tension. Furthermore, after correcting for the microscope's depth of focus, the crystal-fluid interface supports a density mismatch as large as 70% of the crystal density as compared with the 10% mismatch seen in rapidly melting suspensions. The lower figure is consistent with observations of weakly first-order melting in purely repulsive systems such as hard sphere suspensions [13]. Finally, the lattice spacing of the long-lived crystallites remains constant throughout the melting process, whereas short-lived crystals expand while melting, as shown in Fig. 5. These observations suggest that the melting in long-lived crystals is limited by kinetics at the crystal-fluid interface while melting in short-lived crystals is diffusion limited.

The latent heat of melting for an ensemble of mutually repelling spheres arises entirely from the configurational entropy of the crystal [14] and should not depend strongly on a suspension's ionic strength. The melting rate then reflects the differing rates for attachment and detachment of spheres to the crystal surface, which in turn are set by the difference in free energy density between the superheated crystal and the surrounding fluid. This difference decreases as a fluid approaches freezing so that the melting rate should be smaller for the more strongly interacting fluid. Indeed spheres are observed to rejoin the crystal in the slowly melting system as would be required for this scenario. How such a mechanism can support the large crystal-fluid density mismatch remains to be elucidated.

Recent measurements [15] have provided direct evidence for an attractive component in the long-range interaction between like-charged pairs of spheres confined by glass walls. Such an attraction would seem to account naturally for the stability of the metastable crystallites. Attractive interactions also have been proposed to explain a variety of otherwise puzzling phenomena in bulk colloidal suspensions [16]. However, attractive in-

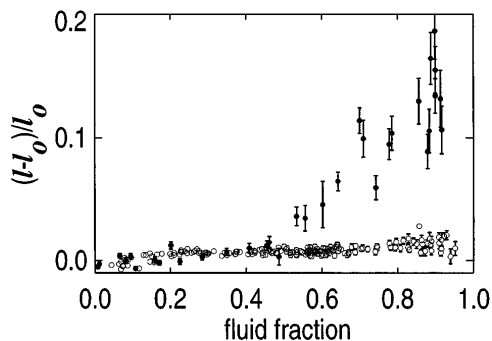


FIG. 5. Evolution of the core crystal lattice constant during melting. The mean nearest-neighbor spacing l relative to the lattice constant during compression, l_0 , appears as a function of the areal fluid fraction. Filled circles correspond to the rapidly melting run in Fig. 4 and open circles correspond to the run with metastable crystallites.

teractions are measured to be strongest for systems with moderate ionic strengths and are not evident [15,17] at the low ionic strength for which we observe metastable crystallites. The question remains then as to the origin of the energy barrier to melting of the metastable crystals.

It is a pleasure to acknowledge valuable conversations with John Crocker, Stuart Rice, Andrew Marcus, David Oxtoby, and Cherry Murray. This work was supported in part by the National Science Foundation under Grant No. DMR-9320378 and in part by the MRSEC Program of the National Science Foundation under Award No. DMR-9400379.

-
- [1] D. J. W. Aastuen, N. A. Clark, L. K. Cottler, and B. J. Ackerson, *Phys. Rev. Lett.* **57**, 1733 (1986); D. G. Grier and C. A. Murray, *J. Chem. Phys.* **100**, 9088 (1994); J. A. Weiss, D. W. Oxtoby, D. G. Grier, and C. A. Murray, *J. Chem. Phys.* **103**, 1180 (1995).
 - [2] C. A. Murray, W. O. Sprenger, and R. A. Wenk, *Phys. Rev. B* **42**, 688 (1990).
 - [3] B. V. Derjaguin and L. Landau, *Acta Physicochim. URSS* **14**, 633 (1941); E. J. Verwey and J. T. G. Overbeek, *Theory of the Stability of Lyophobic Colloids* (Elsevier, Amsterdam, 1948).
 - [4] B. J. Ackerson and P. N. Pusey, *Phys. Rev. Lett.* **61**, 1033 (1988); W. Xue and G. S. Grest, *Phys. Rev. Lett.* **64**, 419 (1990).
 - [5] A. Chowdhury, B. J. Ackerson, and N. A. Clark, *Phys. Rev. Lett.* **55**, 833 (1985).
 - [6] L. M. Milne-Thomson, *Theoretical Hydrodynamics* (Macmillan, New York, 1955).
 - [7] J. Happel and H. Brenner, *AIChE J.* **3**, 506 (1957).
 - [8] B. I. Halperin and D. R. Nelson, *Phys. Rev. Lett.* **41**, 121 (1978); D. R. Nelson and B. I. Halperin, *Phys. Rev. B* **19**, 2457 (1979).
 - [9] F. P. Preparata and M. I. Shamos, *Computational Geometry* (Springer-Verlag, New York, 1985).
 - [10] A. van Blaaderen and P. Wiltzius, *Science* **270**, 1177 (1995).
 - [11] J. C. Crocker and D. G. Grier, *J. Colloid Interface Sci.* **179**, 298 (1996).
 - [12] H. Löwen, T. Palberg, and R. Simon, *Phys. Rev. Lett.* **70**, 1557 (1993).
 - [13] W. B. Russel, D. A. Saville, and W. R. Schowalter, *Colloidal Dispersions* (Cambridge University Press, Cambridge, 1989).
 - [14] W. G. Hoover and F. H. Ree, *J. Chem. Phys.* **49**, 3609 (1968).
 - [15] G. M. Kepler and S. Fraden, *Phys. Rev. Lett.* **73**, 356 (1994); M. D. Carbajal-Tinoco, F. Castro-Román, and J. L. Arauz-Lara, *Phys. Rev. E* **53**, 3745 (1996).
 - [16] N. Ise and H. Yoshida, *Acc. Chem. Res.* **29**, 3 (1996).
 - [17] J. C. Crocker and D. G. Grier, *Phys. Rev. Lett.* **73**, 352 (1994).